

Laboratory for Electrical Instrumentation and Embedded Systems
IMTEK – Department of Microsystems Engineering
University of Freiburg
Sensors Lab Course
Winter term 2022/23

Lab Report M2

Magnetic Sensors

Onur Altinordu (5250773)
January 12, 2023



Data generated in a team together with

Onur Altinordu (5250773)

Shweta Kempipatil (5367928)

1. Introduction

The Earth has a natural magnetic field that is generated by the motion of molten iron in its core. It is similar to that of a bar magnet, with north and south poles, and it extends out into space, creating a region called the magnetosphere. The magnetic field is generated by the motion of molten iron in the outer core of the Earth, which is in a liquid state and therefore able to move around. This motion creates electric currents, which in turn generate magnetic fields [8].

The Earth's magnetic field is not a perfect dipole, and it has several regions of different intensities and directions. It is strongest near the Earth's poles and weakest near the equator. The field is also distorted by solar wind and other factors, resulting in the formation of magnetic fields [8].

The magnetic field has changed over time. It fluctuates regularly, with the field's strength and direction changing over time, and it has also reversed its polarity multiple times in the past. The magnetic field is also currently weakening, with the strength at the earth's surface dropping by about 15% over the past two centuries. It is certainly not fixed and it's expected to weaken further in the coming centuries before eventually reversing polarity which is known as a geomagnetic reversal. And this process takes thousands of years to complete [1].

The Earth's magnetic field serves many important functions, including protecting the planet from harmful solar radiation and helping to direct and stabilize the movement of the atmosphere and oceans. It also plays a role in the formation of auroras and helps animals such as birds and mammals navigate [8], contrary to us humans, who are not able to sense the magnetic field. For this reason, we need devices such as magnetic sensors to be able to measure the magnetic field.

2. Theory

The Hall sensor is a device that measures the magnitude of a magnetic field. It works on the principle of the Hall effect, which states that a voltage difference is generated perpendicular to an electric current in a magnetic field. Hall sensors are used in a variety of applications, such as detecting the position of a rotating object, measuring magnetic field strength, and switching electrical circuits based on the presence or absence of a magnetic field. [9]

The Hall effect is a phenomenon that occurs in certain materials, in which a voltage difference is generated perpendicular to an electric current in a magnetic field. The Hall voltage is proportional to the magnetic field strength and can be used to measure the magnetic field or to detect the presence of a magnetic field. [10]

When working with magnetometers, dealing with uncalibrated sensor values can be very challenging. Therefore, before even starting any measurements, the sensor must be calibrated. A sensor model must be developed to mathematically correct sensor measurements for various error sources. A magnetometer can be modeled as follows [2]:

$$\tilde{\mathbf{m}} = SI^{-1}(\mathbf{m}_E + \mathbf{m}_{e(t)}) + \mathbf{b}_{HI} + \mathbf{m}_{i(t)}$$

Equation 1 [2]

Where the measurement vector (\mathbf{m}) is a combination of Earth's magnetic field and magnetic fields caused by nearby disturbances. By using this measurement model, a compensation model can be

created to account for the hard iron (bHI) and soft iron (SI) distortions in the local magnetic field resulting from internal, non-time-varying magnetic disturbances [2].

$$\mathbf{m}_c = S_I(\tilde{\mathbf{m}} - \mathbf{b}_{HI})$$

$$\begin{bmatrix} m_{c_x} \\ m_{c_y} \\ m_{c_z} \end{bmatrix} = \begin{bmatrix} C_{00} & C_{01} & C_{02} \\ C_{10} & C_{11} & C_{12} \\ C_{20} & C_{21} & C_{22} \end{bmatrix} \begin{bmatrix} \tilde{m}_x - b_{H_0} \\ \tilde{m}_y - b_{H_1} \\ \tilde{m}_z - b_{H_2} \end{bmatrix}$$

Equation 2 [2]

Different variables may distort the magnetometer readings. These variables are hard-iron and soft-iron distortions. Hard-iron distortions are caused by objects that generate a magnetic field and soft-iron distortions are occurring because of the changes in the existing magnetic field. These distortions can stretch or change the magnetic field depending on the direction in which the field is acting in relation to the sensor [2].

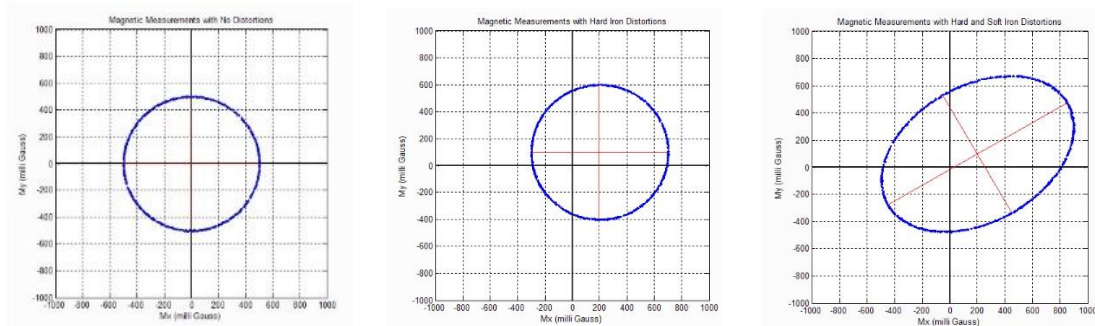


Figure 1 – Magnetometer Measurements [2]

When magnetic readings on the x and y axes are plotted, they create a circular shape. Without any bias, the shape looks like a perfect circle at the origin. When a hard-iron distortion is present, the center of the circle is shifted from the center as can be seen from the plot in the middle of Figure 1. Soft-iron distortion has a different effect. As can be seen from the rightmost plot in Figure 1, the center of the circle is shifted and the circular shape is stretched into an ellipsoid. This is because both hard-iron and soft-iron distortions are affecting the magnetic field readings.

Hard-iron matrix parameters are set so that the center of the plot is set back to the origin and soft-iron parameters are chosen to turn the ellipsoid back into a circle. motionCal [3] software developed by PJRC is a tool that helps the user visualize the magnetic field and determines hard-iron and soft-iron parameters that are used in the calibration of the magnetic sensor.

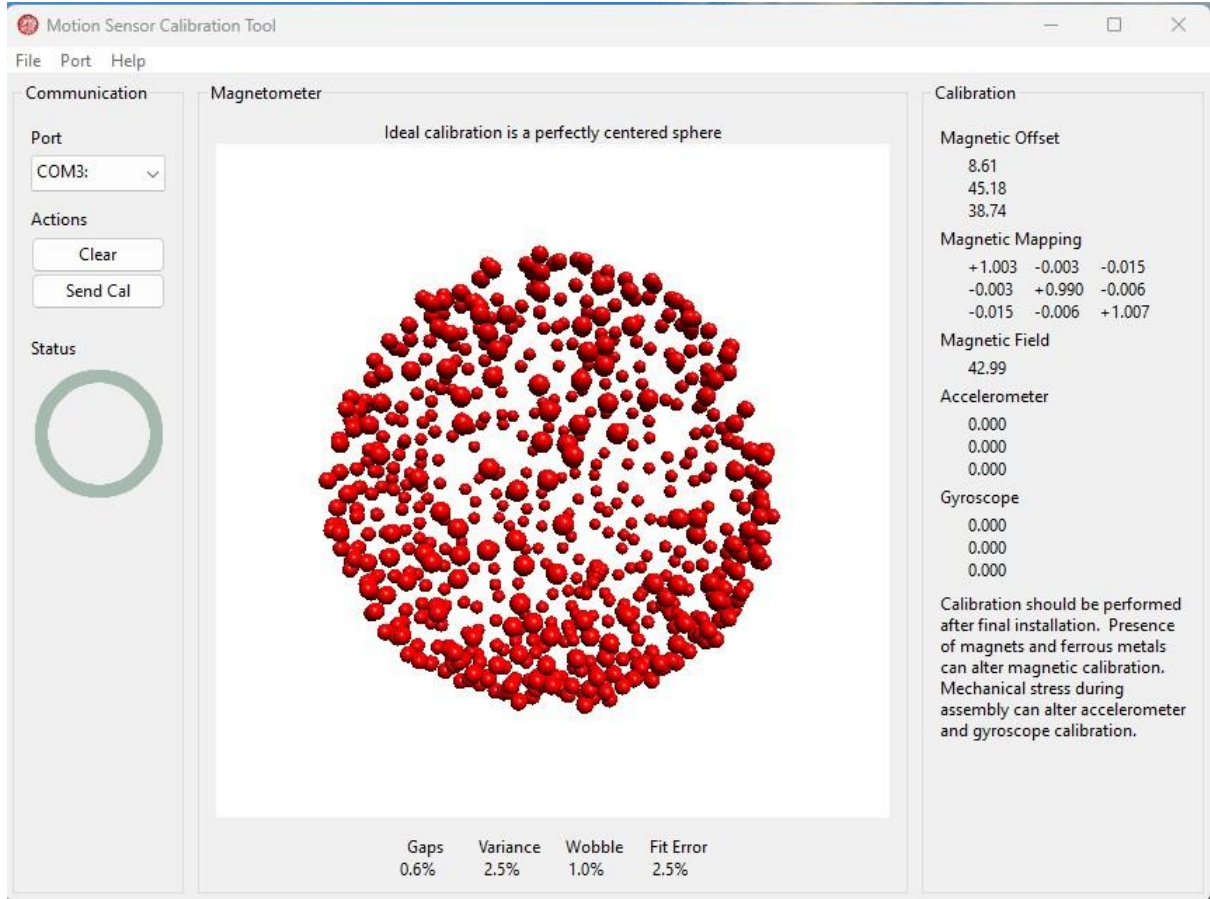


Figure 2 – Determining hard-iron & soft-iron parameters using motionCal software

To determine the parameters, the sensor readings are passed to the motionCal in CSV (comma-separated-values) format. The sensor is then moved and rotated in every direction until a sphere with very few gaps form.

At specific locations, the strength of the Earth's magnetic field is measured by three components: the horizontal component, the vertical component, and the overall intensity. All three components are shown below:

- Horizontal Magnetic Field Intensity: $B_{hor} = \sqrt{B_x^2 + B_y^2}$
- Vertical Magnetic Field Intensity: $B_{vert} = B_z$
- Total Magnetic Field Intensity: $B_{tot} = \sqrt{B_x^2 + B_y^2 + B_z^2}$

These components will, later on, be calculated using the measurements and will be compared to the earth's magnetic field model.

For the magnetometer to be able to work as a compass, the heading must be calculated. Equation 3 gives the degrees relative to the north direction:

$$Heading = -\frac{180}{\pi} \times \tan^{-1} \frac{B_x}{B_y}$$

Equation 3 [2]

Equation 3 results in 0° when the y-axis of the magnetometer is perfectly aligned with the magnetic north.

If one needs to calculate the true north, then one must add the magnetic declination to the heading value. The magnetic declination can be found on the NOAA website. However, the magnetic declination is given in degrees and minutes format. Therefore it should be converted into the degree format.

$$Dec = S \times \left(degrees + \frac{minutes}{60} \right); S = \begin{cases} +1 & \text{if East} \\ -1 & \text{if West} \end{cases}$$

Equation 4 [2]

When the result of Equation 4 is added to Equation 3, degrees to the true north can be calculated.

3. Methods

In this module, the BMM150 [4] sensor on the Arduino Nicla Sense ME board will be utilized to measure the magnetic field of the Earth.

The BMM150 is a sensor manufactured by Bosch Sensortec . It is a geomagnetic sensor that is designed to detect the strength and direction of the Earth's magnetic field. The sensor features a triaxial magnetometer, which can measure the magnetic field in three dimensions (x, y, and z) with high accuracy and resolution.

One of the main features of this sensor is the low power consumption and a wide magnetic field range ($\pm 1300 \mu\text{T}$ (x, y-axis) $\pm 2500 \mu\text{T}$ (z-axis)). It also has high performance and stability even under the influence of external interference fields. The sensor has a small size, measuring 1.56 mm x 1.56 mm x 0.6 mm, making it well-suited for embedded applications.

For this experiment, an Arduino Nicla Sense ME is connected to a battery-powered notebook via USB. The notebook is used as both a power supply and a data logger. The board was programmed using the Arduino IDE with the Arduino_BHY2 library version 1.5 (Bosch Sensortec). motionCal was used for sensor calibration and Excel Data Streamer was used for data logging. To find the north direction, Google Earth Pro was used.

Two Arduino programs were utilized to complete the experiment. The first program is for passing raw sensor data to the motionCal software. After the calibration matrices (hard iron & soft iron) were obtained from the motionCal, they are manually entered into the second program. The second program is for calibrating the sensor and for passing the calibrated measurements to Excel Data Streamer for data logging every 100 ms. Each experiment goes on until 1000 measurements are collected. Indoor experiments were done on the first and second floor of Universitätsbibliothek Freiburg and the outdoor experiment was done at Platz der Alten Synagoge. The interpretation of the collected measurements was done using Excel.

4. Results and Discussion

4.1 Task 1

On the first task of the experiment, the BMM150 sensor was held stationary and 1000 magnetic field intensity measurements for all three axes were taken. In the following part, these measurements will be plotted and interpreted.

4.1.1 Part a)

After calibrating the sensor with the help of motionCal software, magnetic field intensity measurements for the x, y, and z axes were taken. As can be observed from Figures 3, 4, and 5, there is no drift since the linear fit depicted with an orange line does not deviate from the initial value after 1000 measurements for all of the axes.

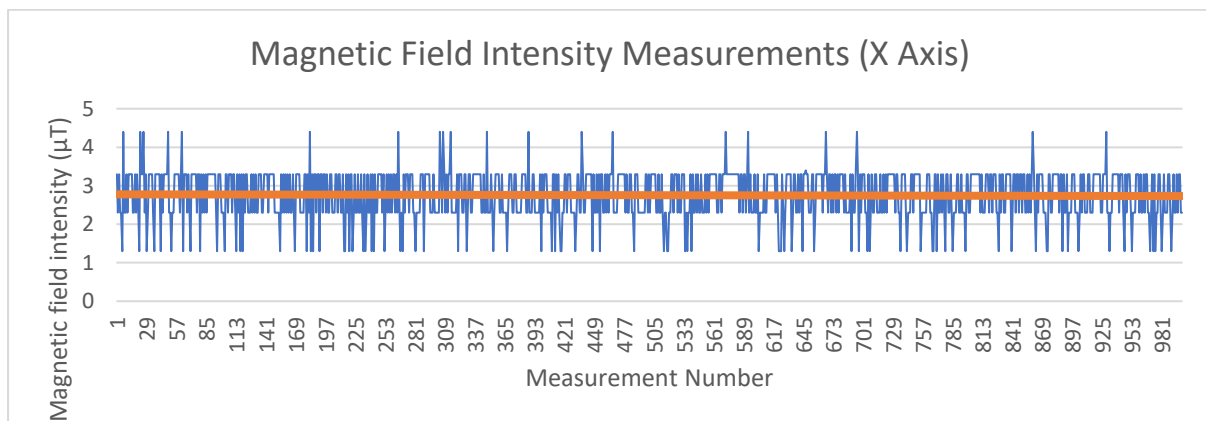


Figure 3 – Intensity measurements x-axis

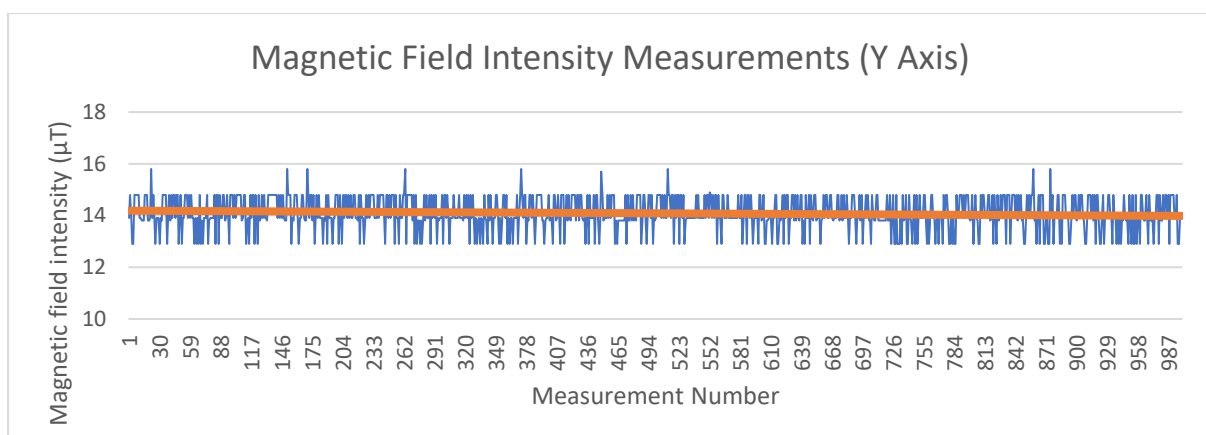


Figure 4 – Intensity measurements y-axis

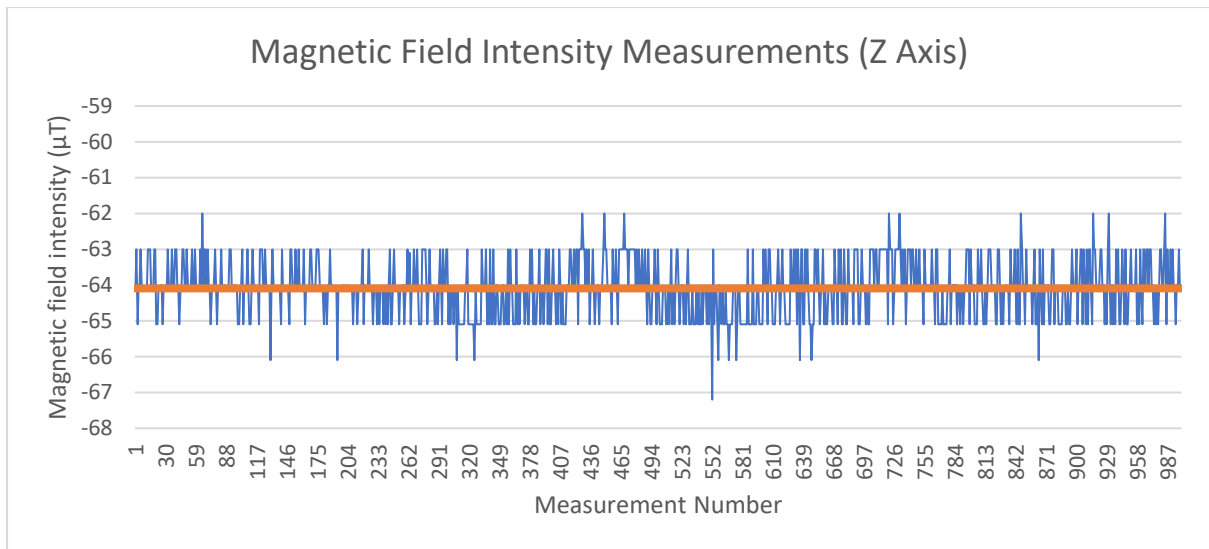


Figure 5 – Intensity measurements z-axis

4.1.2 Part b)

The average of all three axes was calculated. The mean is $2,8 \mu\text{T}$ for the x-axis, $14,0 \mu\text{T}$ for the y-axis, and $-64,1 \mu\text{T}$ for the z-axis. In Figures 6, 7, and 8, histograms of subtracted means can be observed.

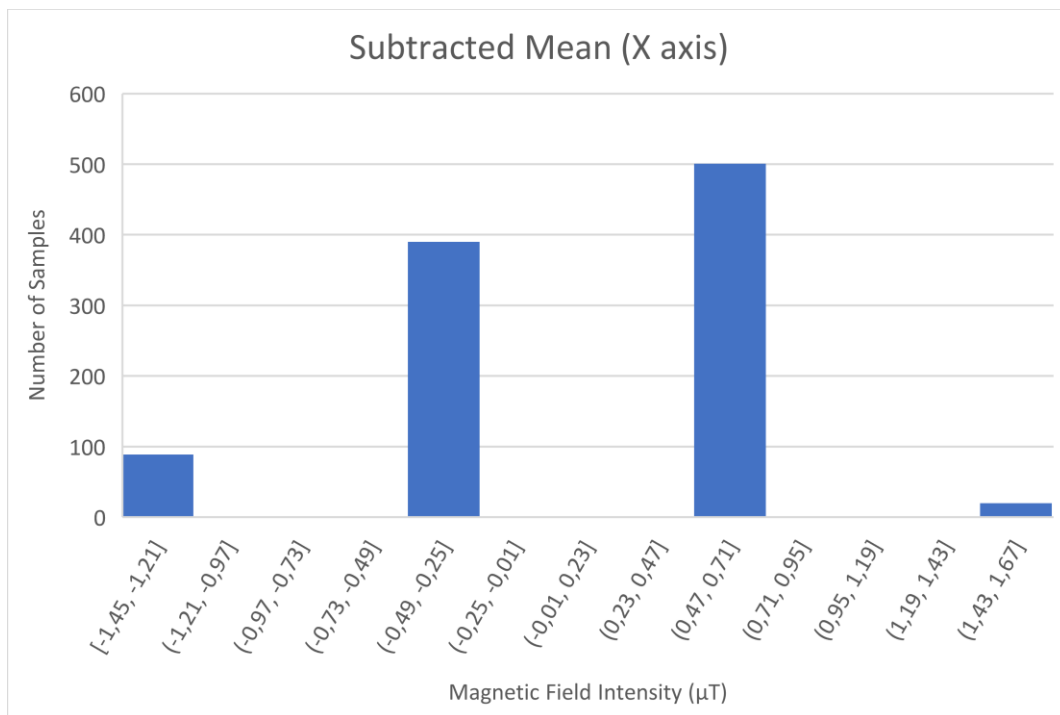


Figure 6 – Histogram of the subtracted mean x-axis

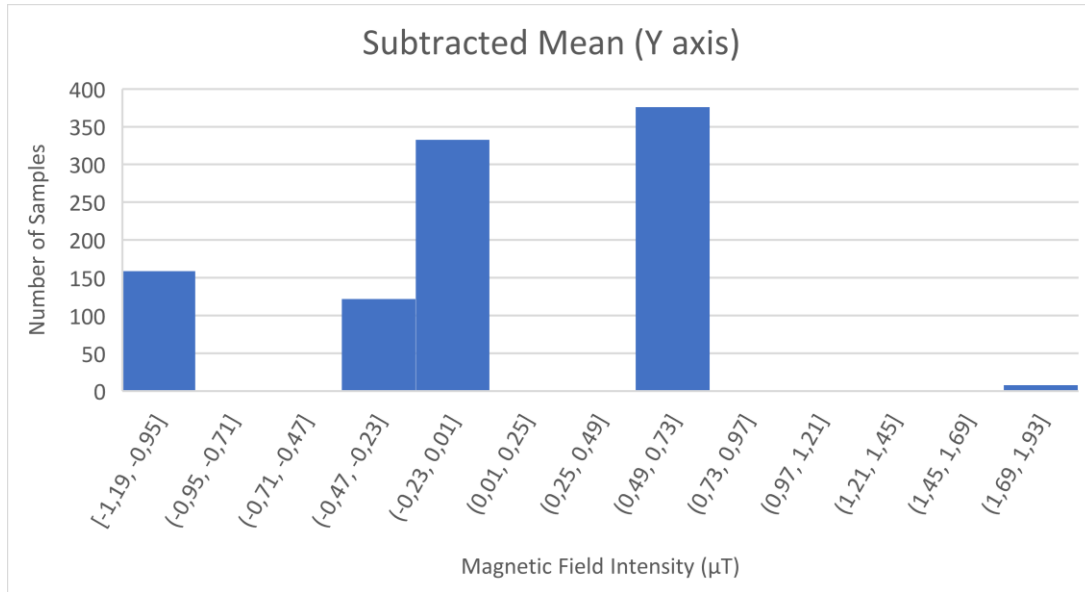


Figure 7 – histogram of the subtracted mean y-axis

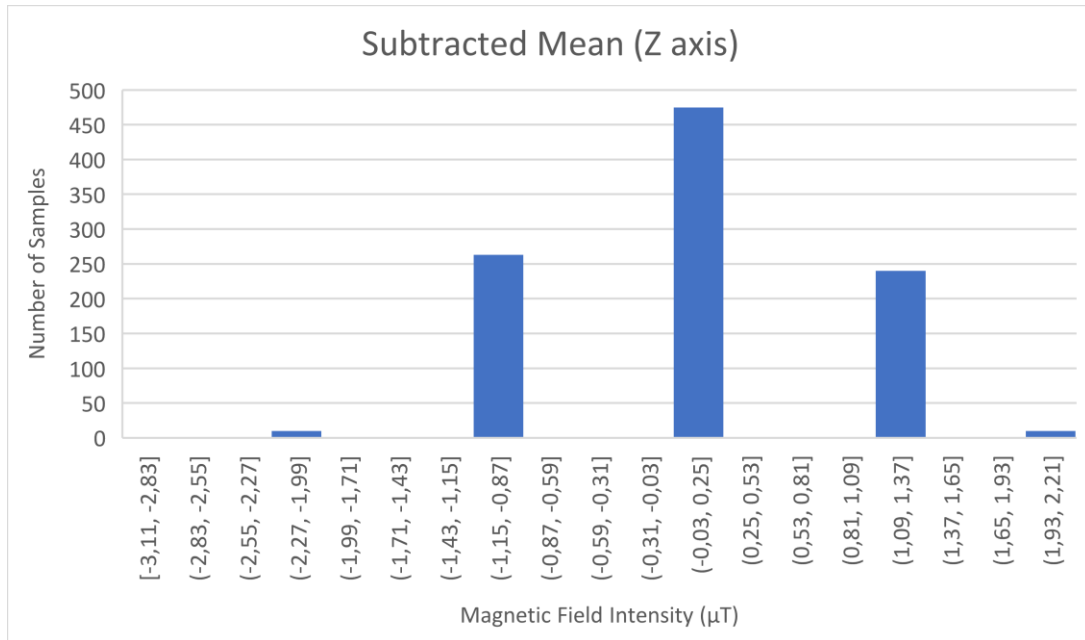


Figure 8 – Histogram of the subtracted mean z-axis

When histograms for all three axes are observed, it can be deduced that the Hall sensor distribution is concentrated around the mean value more and it is closer to the gaussian distribution in comparison to the FlipCore elements.

	X-Axis	Y-Axis	Z-Axis
Mean	$-2,5 \times 10^{-14} \mu\text{T}$	$2,3 \times 10^{-13} \mu\text{T}$	$-6,6 \times 10^{-13} \mu\text{T}$
Standard Deviation	0,7 μT	0,7 μT	0,8 μT

Table 1 – Means and Standard deviations of all axes

4.2 Task 2

For this task, 1000 magnetic field intensity measurements were taken for all three axes, and the measurements were repeated after the board was flipped around the x and y axes. These measurements are then used to calculate the offset value for all axes.

4.2.1 Part a, b & c)

The mean values of all axes before and after the board was flipped on the x and y axes, and their offsets can be observed in Table 2 below. Ideally, only the sign of the measurements should be changed once the board is flipped. Therefore, the absolute value of the difference between the measurements before and after the board is flipped is equal to the offset.

	Field Intensity (x-axis)	Field Intensity (y-axis)	Field Intensity (z-axis)
Before the board is flipped around x and y axes	11,3 μT	9,4 μT	-65,5 μT
After the board is flipped around x and y axes	-10,0 μT	-15,2 μT	-63,2 μT
Offset	1,3 μT	5,8 μT	2,3 μT

Table 2 – Magnetic field intensity measurements

4.3 Task 3

The following parts of the experiment were done outdoors to avoid the interference of local magnetic fields. The vicinity of Universitätsbibliothek Freiburg was chosen for the task.

4.3.1 Part a)

Measurements for all three axes were repeated once more outdoors. The measurement results with their corresponding standard deviations are shown below in Table 3:

Field Intensity (x-axis)	Field Intensity (y-axis)	Field Intensity (z-axis)
-23,4 $\mu\text{T} \pm 0,6 \mu\text{T}$	16,0 $\mu\text{T} \pm 0,5 \mu\text{T}$	-39,5 $\mu\text{T} \pm 0,4 \mu\text{T}$

Table 3 – Outdoor measurement results

4.4 Task 4

The geomagnetic model for the experiment location was taken from the NOAA website [5].

4.4.1 Part a)

In Table 4, The horizontal, vertical, and total magnetic field intensities are shown. These values are derived according to the Equations given in section 2. First, these values were calculated using the maximum and minimum of the 1000 measurements for each axis to have an idea about the precision. Then, they were calculated again using the mean value of all measurements for every axis. These intensities are then compared to the intensities of the geomagnetic model.

	Measurement (Max)	Measurement (Min)	Difference (Max, Min)	Measurement (Mean)	Geomagnetic Model	Difference (Mean, Model)
B_{hor}	30,8 μT	25,8 μT	5,0 μT	28,3 μT	21,2 μT	7,1 μT
B_{vert}	41,5 μT	37,4 μT	4,1 μT	39,5 μT	43,5 μT	3,9 μT
B_{tot}	51,7 μT	45,4 μT	6,3 μT	48,7 μT	48,4 μT	0,3 μT

Table 4 - Comparison of calculations with the geomagnetic model

4.4.2 Part b)

The Zero-B offset is given as $\pm 40 \mu\text{T}$ [6] in the specification section of the BMM150 datasheet. When the Difference (Mean, Model) column of Table 4 is inspected, it can be seen that the offsets are well below this value and they are very close to the geomagnetic model values. Therefore, the measurement fits with the real values. Moreover, it can be said that the measurements are very precise, considering the difference between the maximum and the minimum intensity values.

4.5 Task 5

On the final task, the BMM150 magnetometer was used as a compass. The experiment was done at Platz der Alten Synagoge shown in Figure 10 below:



Figure 9 – The location and direction of the experiment are depicted with the red arrow

4.5.1 Part a)

1000 measurements were taken and the mean of the magnetic field intensities of the x and y axes was calculated. These intensities are then used to calculate the heading value as described in Equations 3 and 4. The magnetic field intensity and the heading values are shown in Table 4 below:

Field Intensity (x-axis)	Field Intensity (y-axis)	Heading (Degrees from the North direction)
0,06 μT	28,6 μT	2,9°

Table 4 – Magnetic field intensities and degrees from north

4.5.2 Part b)

Considering the human error too, 2,9° degrees of deviation from the true north is very accurate and acceptable. Since the heading value also includes the declination taken from the NOAA website, the results show the true north. If the program was able to take the magnetic declination from the internet, it would always be able to show the true north even if the earth's magnetic field changed at that location. Currently, the declination for the given location is 3.1° degrees.

5. Summary

In this experiment, BMM150 magnetic sensor was tested and its offset values were calculated. The data were normally distributed. Then, the board was taken outside. The measurements that are done outside are then compared to the values taken from the NOAA website. The values at the NOAA fit the measurements. Finally, the sensor was programmed to work like a compass and its accuracy and precision were discussed. The sensor was very successful at determining the real North direction. After this experiment, it can easily be said that the BMM150 magnetometer is a very accurate and precise sensor.

6. References

- [1] *Swarm probes weakening of Earth's magnetic field* (2020) ESA. Available at: https://www.esa.int/Applications/Observing_the_Earth/FutureEO/Swarm/Swarm_probes_weakening_of_Earth_s_magnetic_field (Accessed: January 13, 2023).
- [2] *Magnetometer hard & Soft Iron Calibration* (no date) VectorNav. Available at: <https://www.vectornav.com/resources/inertial-navigation-primer/specifications--and--error-budgets/specs-hsicalibration> (Accessed: January 13, 2023).
- [3] *Motion Sensors* (no date) PJRC. Available at: https://www.pjrc.com/store/prop_shield.html (Accessed: January 13, 2023).
- [4] *Magnetometer BMM150* (no date) Bosch Sensortec. Available at: <https://www.bosch-sensortec.com/media/boschsensortec/downloads/datasheets/bst-bmm150-ds001.pdf> (Accessed: January 13, 2023).
- [5] Center, N.G.D. (no date) *NCEI geomagnetic calculators, NCEI Geomagnetic Calculators*. U.S. Department of Commerce. Available at: <https://www.ngdc.noaa.gov/geomag/calculators/magcalc.shtml> (Accessed: January 13, 2023).
- [6] *Bosch Sensortec* (no date). Available at: <https://www.bosch-sensortec.com/media/boschsensortec/downloads/datasheets/bst-bmm150-ds001.pdf> (Accessed: January 13, 2023).
- [7] Hymel, S. (no date) *How to calibrate a magnetometer*, DigiKey. Available at: <https://www.digikey.com/en/maker/projects/how-to-calibrate-a-magnetometer/50f6bc8f36454a03b664dca30cf33a8b> (Accessed: January 13, 2023).
- [8] *Earth's magnetic field* (2022) Wikipedia. Wikimedia Foundation. Available at: https://en.wikipedia.org/wiki/Earth's_magnetic_field?oldformat=true (Accessed: January 13, 2023).
- [9] *Hall effect sensor* (2021) Wikipedia. Wikimedia Foundation. Available at: https://en.wikipedia.org/wiki/Hall_effect_sensor?oldformat=true (Accessed: February 4, 2023).
- [10] *Hall effect* (2023) Wikipedia. Wikimedia Foundation. Available at: https://en.wikipedia.org/wiki/Hall_effect?oldformat=true (Accessed: February 4, 2023).